The response of household debt to COVID-19 using a neural networks VAR in OECD.

Emmanuel C. Mamatzakis[a], Steven Ongena[b] and Mike G. Tsionas[c]

May 2022

Abstract

This paper investigates responses of household debt to COVID-19 related data like confirmed cases and confirmed deaths within a neural networks panel VAR for OECD countries. Our model also includes a plethora of non-pharmaceutical and pharmaceutical interventions. We opt for a global neural networks panel VAR (GVAR) methodology that nests all OECD countries in the sample. Because linear factor models are unable to capture the variability in our data set, the use an artificial neural network (ANN) method permits to capture this variability. The number of factors, as well as the number of intermediate layers, are determined using the marginal likelihood criterion and we estimate the GVAR with MCMC techniques. We also report δ-values that capture the dominance of each individual country in the network. In terms of dominant countries, UK, USA, and Japan dominate interconnections within the network, but also countries like Belgium, Netherlands, and Brazil. Results reveal that household debt positively responds to COVID-19 infections and deaths. Lockdown measures such as stay-at-home advice, and closing schools, all have a positive impact on household debt, though they are of transitory nature. However, vaccinations and testing appear to negatively affect household debt.

Keywords: COVID-19, household debt, ANN, panel VAR, MIDAS, OECD.

JEL Classifications: C32, E44, F44.

[a] Professor of Finance, Department of Management, Birkbeck, University of London, Malet Street, Bloomsbury, London WC1E 7HX, UK. E-mail: e.mamatzakis@bbk.ac.uk. [b] Professor of Finance, Department of Banking and Finance, University of Zurich, Zurich 8032, Switzerland; Swiss Finance Institute; KU Leuven; NTNU Business School; and CEPR. Email: steven.ongena@bf.uzh.ch. [c]Professor of Economics and Econometrics, Lancaster University Management School, Bailrigg, Lancaster, LA1 4YX, UK. E-mail: m.tsionas@lancaster.ac.uk. Ongena acknowledges financial support from ERC ADG 2016 - GA 740272 lending. The Authors acknowledge financial support from ESRC ES/V015826/1.

1. Introduction

The paper sheds light on household financial behaviour in relation to household debt during the pandemic to inform policy making interventions and economic recovery. We investigate the responses of household debt in OECD countries to shocks in COVID-19 related data like confirmed cases and confirmed deaths within a neural networks panel VAR. We provide evidence that disentangles the impact of the pandemic and government interventions on household debt in the OECD.

The importance of household debt for macroeconomic and financial stability is unequivocal. Zabai (2020) and OECD (2020) report recent data that show that household consumption is about 60 percent of GDP in OECD whereas household debt, mostly in the form of mortgages, captures up to 40 percent of banks' asset. Franklin et al. (2021) presented descriptive analysis to argue that many UK households have managed to weather the crisis of COVID-19, though the Authors also argue that households with unsecured loans could face financial difficulties. Georgarakos, and Kenny (2022), using a new consumer expectations survey data for EU, show that policy makers by clearly communicating their COVID-19 interventions (see Christelis, et al. 2020), i.e., fiscal measures, would enhance consumers perception about the adequacy of these interventions and thereby they would incentivise household spending, including debt payment.[1] Kubota et al. (2021) employ a natural experiment in Japan to show that household would increase their spending as response to COVID-19 pandemic governments interventions that take the form of cash transfers (see also Chetty et al. 2020 for US; and Carvalho, et al. 2020 for UK).

This paper builds on the above empirical studies to provide evidence of responses of household debt, in particular, to shocks due to the pandemic within a unique panel global Vector Autoregressive model that nests neural networks and postulates forecasts over 24 months period under various COVID-19 scenarios while controlling for non-pharmaceutical and pharmaceutical interventions as shocks in the GVAR. For example,

[1] Identifying consumer perceptions is beyond the scope of the current paper due to data availability issues but it is worth noting recent research of Roth and Wohlfart (2020) and Roth et al. (2021) that show most households in US underestimate the federal debt to GDP and once they are informed their perceptions change against raising government spending. This is of some significance as the COVID-19 crisis poses further challenges to governments interventions and fiscal imbalances.

government interventions in the form of lockdowns play a prominent role in our modelling. Because linear factor models may be unable to capture the variability in the data, we use an artificial neural network (ANN) method. The number of factors as well as the number of intermediate layers are determined using the marginal likelihood criterion and we estimate the GVAR with MCMC techniques. We also employ Mixed Data Sampling (MIDAS) that allows the use of data of different frequencies and identifies household debt responses under different COVID-19 scenarios. Note that household and macroeconomic data in OECD are country specific on annual frequency while COVID-19 related data are on a daily frequency. Also, we provide a detailed map of interconnectedness of the underlying causal nodes of various contributing factors to household finances as well as interactions between household debt repayment, relating comparisons between UK and advanced countries. We, therefore, follow Pesaran and Yang (2016) to identify 'strong' and 'weak' dominant countries in the network based in measures of eigenvector degrees and centrality of Acemoglu et al. (2012). To this end, we estimate pervasiveness scores to identify the dominant countries in OECD. Last, we rank the principal contributing factors to household debt repayment so to inform policy makers to prioritise actions on specific factors.

Results reveal that household debt positively responds to COVID-19 infections and death. Lock down measures such as stay at home advise, closing schools, all have a positive impact on household debt repayments in GVAR, though of transitory nature. However, pharmaceutical interventions like vaccinations and testing appear to negatively affect household debt. In terms of dominant countries, UK, USA, and Japan dominate interconnections within the network, but also countries like Belgium, Netherlands, and Brazil.

In what follows Section 2 presents the ANN GAVR. Section 3 reports the data set and provides descriptive statistics. Section 4 discusses results. The last section presents some concluding remarks.

2. The global VAR model

Suppose $Y_t = [y_{1,t}, y_{2,t}, \ldots, y_{n,t}]'$ is an $n \times 1$ vector time series which can be

described by a vector autoregression (VAR):

$$Y_t = BY_{t-1} + \varepsilon_t, t = 1, \ldots, T, \tag{1}$$

where $\varepsilon_t \sim \mathcal{N}_n(\mathbf{0}, \Omega)$. Following previous contributions (Koop, Korobilis and Pettenuzzo, 2017, Primiceri, 2005, Eisenstat, Chan and Strachan, 2016 and Carriero, Clark and Marcellino, 2015) we use a triangular decomposition of Ω as follows:

$$A\Omega A' = \Sigma\Sigma, \tag{2}$$

where $\Sigma = \mathrm{diag}[\sigma_1, \ldots, \sigma_n]$, and A is a lower triangular matrix with ones on the main diagonal. Define $A = I_n + \tilde{A}$, where $\tilde{A}$ is a lower triangular matrix with zeros on the main diagonal. Therefore, we can write the VAR as follows:

$$Y_t = BY_{t-1} + A^{-1}\Sigma\xi_t, \tag{3}$$

where $\xi_t \sim \mathcal{N}_n(0, I_n)$.

In turn, we can write:

$$Y_t = \Theta Z_t + \Sigma\xi_t, \tag{4}$$

where $\Theta = \left[\Gamma, \tilde{A}\right]$ and $\Gamma = AB$. The advantage of the representation is that this is a recursive system. The first equation involves only Y_{t-1}, the second equation includes $(Y'_{t-1}, -y_{1,t})$, the third equation includes $(Y'_{t-1}, -y_{1,t}, -y_{2,t})$ etc. Moreover, $\tilde{A}$ controls for the error covariances.

2.1. The artificial neural network (ANN)

In GVARs it is typical that various VARs are connected through some observed variables like an export / import index converted to lie between zero and one. Here, we connect the different VARs through several common dynamic factors (an $M \times 1$ vector, f_t). The VAR model for each country, is as follows.

$$Y_t^{(c)} = B^{(c)} Y_{t-1}^{(c)} + \Delta^{(c)} Z_t^{(c)} + \varepsilon_t^{(c)}, t = 1, \ldots, T, \tag{5}$$

where $\varepsilon_t^{(c)} \sim \mathcal{N}_n(\mathbf{0}, \Omega^{(c)})$, for country $c \in \{1, \ldots, C\}$,and Z_t is a $K \times 1$ vector of covariates whose coefficients are given in the $n \times K$ matrix Δ.

We suppose that the dynamic factors are given as:

$$f_t = \Lambda f_{t-1} + u_t, \tag{6}$$

where Λ is an $M \times M$ matrix of unknown coefficients, and $u_t \sim \mathcal{N}_M(0, V)$, where V is an unknown covariance matrix, assumed to be diagonal with different elements along the main diagonal. As linear factor models may be unable to capture the variability in the data, we use an artificial neural network (ANN):

$$f_t = \Lambda f_{t-1} + \sum_{g=1}^{G} a_g \, \varphi(b_g f_{t-1}) + \varepsilon_t, \tag{7}$$

where a_g and b_g are unknown parameters, $\varphi(z) = \frac{1}{1+e^{-z}}$ is the logistic activation function, and G is the unknown number of components in the ANN. The number of factors M as well as the number of intermediate layers (G) are determined using the marginal likelihood criterion (Diccio et al., 1997). We use the MCMC technique in Appendix A.1. We use 150,000 iterations, the first of which are discarded to mitigate possible start up effects.

In turn, we modify (5) as follows:

$$Y_t^{(c)} = B^{(c)} Y_{t-1}^{(c)} + \Delta^{(c)} Z_t^{(c)} + \Phi^{(c)} f_t + \varepsilon_t^{(c)}, t = 1, \ldots, T, \tag{8}$$

where $\varepsilon_t^{(c)} \sim \mathcal{N}_n(\mathbf{0}, \Omega^{(c)})$, and $\Phi^{(c)}$ is an $n \times M$ matrix of unknown coefficients. So, we couple the dynamic factor model in (7) with the VAR models in (5). In our case, the vector Y_t contains household debt, household savings, household spending, GDP,

exchange rate, government deficit, share prices, and the long-term interest rate (n=8). For each country, the VAR can be estimated on an equation-by-equation basis resulting in substantial reduction in computation time. The dynamic factors in (6) are computed beforehand to simplify computations so, for all equations of the GVAR as well as different countries, equations can be estimated on an equation-by-equation basis.

We use a flat prior for the coefficients in (7). For the diagonal elements of $A^{(c)}$ we assume that they are normally distributed with mean 1 and standard deviation 0.2. The non-diagonal elements have a normal prior with mean zero and standard deviation 0.2. For the elements of $\Delta^{(c)}$ and $\Phi^{(c)}$ we assume that they have a standard normal distribution. Suppose that the jth typical equation of (8) has the form

$$Y_{t,j}^{(c)} = B_j^{(c)'} Y_{t-1}^{(c)} + \Delta_j^{(c)'} Z_t^{(c)} + \Phi_j^{(c)'} f_t + \varepsilon_{t,j}^{(c)}, t = 1, \ldots, T, j = 1, \ldots, 8, \tag{9}$$

where $B_j^{(c)'}, \Delta_j^{(c)}, \Phi_j^{(c)}$ denotes the jth row of matrices $B^{(c)}, \Delta^{(c)}, \Phi^{(c)}$ respectively. We keep in mind that (9) is estimated in the form of (4) so, in fact, the indices are $j \in \{1, \ldots, 8\}$ and $c \in \{1, \ldots, C\}$. As the GVAR can be estimated now for each country and VAR variable on an equation-by-equation basis, implementation of Markov Chain Monte Carlo (MCMC, Geweke, 1999).

2.2. The pervasiveness scores within the ANN

Following from Pesaran and Yang (2016) that identify 'strong' and 'weak' dominant countries in the network based in measures of eigenvector degrees and centrality of Acemoglu et al. (2012), we also estimate δ-values per country in equation (9) (see Pesaran and Yang 2016 and Tsionas et al. 2016). The δ-values captures the dominance of each individual country in the network of Equation (9) whereby if a country has δ-value close to one then that country would be the most dominant in the network. So low δ-values for imply low dominance in the network. Pesaran and Yang (2016) call these δ-values pervasiveness scores.

The covariates $Z_{k,t}^{(c)}$ in (9) are available monthly, whereas the variables in the VARs

are annually observed. Khalaf et al. (2020) propose to follow Ghysels et al. (2004) and use the exponential Almon (1965) lag polynomial of length H (Almon, 1965) defined for the kth variable, as:

$$Z_{k,t}(\vartheta) = \sum_{j=1}^{m} Z_{k,t,j}\, w_{k,j}(\vartheta_k), \tag{10}$$

so, the high-frequency data for a variable $Z_{k,t,j}$ (variable k, year t and date $j = 1,\ldots,m$ are aggregated into the annual variable $z_{i,t}(\vartheta)$, where ϑ is a vector of parameters, and the weights $w_j(\vartheta)$(omitting the variable index, k, for simplicity) are

$$w_j(\vartheta) = \frac{\prod_{h=1}^{H} e^{j^h \vartheta_h}}{\sum_{j=1}^{m}\left(\prod_{h=1}^{H} e^{j^h \vartheta_h}\right)}. \tag{11}$$

Khalaf et al. (2020) set $H = 2$ on the basis that it can model a variety of patterns, see also Ghysels (2016). When $\vartheta_h = 0$ for all h, then all weights are equal to $\frac{1}{m}$. In fact, we can choose the appropriate value of H using the marginal likelihood of the model. The elements of $Z_t^{(c)}$ are vaccine prioritisation, testing policy, confirmed cases, confirmed deaths, vaccination policy, school closing, workplace closing, cancel public events, restrictions on gatherings, close public transport, stay at home requirements, international restrictions, contact tracing, and stringency index. Therefore, instead of (9) we have:

$$Z_{t,k}^{(c)}(\vartheta) = \sum_{j=1}^{m} Z_{k,t,j}\, w_{k,j}(\theta), k = 1,\ldots,14. \tag{12}$$

To simplify the computations, the weighting is performed before estimating the GVAR, using the MCMC technique in Appendix. We use 150,000 iterations, the first of which are discarded to mitigate possible start up effects. In turn, we consider Generalized Impulse Response Functions (GIRFs; Koop et al., 1996; Pesaran and Shin, 1998).

3. The data set.

We draw on three data sources. The non-pharmaceutical interventions data is from the

Oxford COVID-19 Government Response Tracker (OxCGRT) (Hale et al., 2020). The daily COVID-19 case data are from the Johns Hopkins University's Center for Civic Impact. OxCGRT collects publicly available information on 19 indicators of government responses related to containment and closure policies, economic policies, and health system policies, which are combined into four indices ranging from 0 to 100. The indices include the number and strictness of government policies and do not indicate appropriateness or effectiveness response.

Data on government interventions concern three main areas of interventions: a) containment and closure, b) health system, and c) economic stimulus. All the indicators are available on a daily and monthly basis. The containment and closure interventions include eight sub-indicators: i) school closing, ii) workplace closing, iii) cancellation of public events, iv) restrictions on gatherings size, v) public transport closed, vi) stay at home requirements, vii) restrictions on internal movement, and viii) restrictions on international travel. The second area of interventions include health system: i) public information campaigns, ii) testing policy, and iii) contact tracing. Since these policies help to cope with the pandemic quicker, they may be also discounted in stock prices. The third area includes economic stimulus packages such as: income support, and debt or contract relief for households. These stimuluses affect the economy through various channels. For instance, stimulus supports consumption and spending in times of distress; hence, they may significantly affect local equity markets. Finally, besides the individual measures, we also consider the overall Stringency Index by Hale et al. (2020). The index aggregates the data pertaining is re-scaled to create a score between 0 and 100. This index provides a synthetic measure of the intensity of different non-medical government interventions during the pandemic. Table 1 reports the main descriptive statistics of our sample.

In some detail in term of the data, we measure exposure to the pandemic by computing the growth rate of the cumulative number of confirmed cases (and deaths) in each country on daily frequency starting from 1st of January 2020 to end of 2021 (see Table 1 for COVID-19 related data). In some detail, COVID-19 and lock down variables include: vaccines; tests; confirmed deaths; hospitalisations; ICU data; school closing; workplace closing; cancel events; gatherings restrictions; transport closing; stay home

restrictions; internal movement restrictions; international movement restrictions; information campaigns; testing policy; contact tracing; stringency index. All the changes in government policies are tracked daily and monthly. Therefore, when we perform the regressions based on weekly returns, we calculate the weekly averages for the considered period.

Table 1: COVID-19 related data.

	Obs	Mean	Std. DEV	Min.	Max
Vaccine Prioritisation	17,778	0.838227	0.8500284	0	2
Testing Policy	17,760	2.185698	0.871997	0	3
Confirmed Cases	17,388	2496793	7108942	0	7.80E+07
Confirmed Deaths	17,388	51394.35	128410.3	0	925435
MedicallyClinicallyVulner.	17,775	2.106723	2.19719	0	5
VaccinationPolicy	17,775	1.613446	1.021128	0	3
SchoolClosing	17,775	1.687539	0.9258727	0	3
WorkPlaceClosing	17,775	1.510999	0.688261	0	2
CancelPublicEvents	17,775	2.880675	1.419374	0	4
RestrictionsonGatherings	17,775	0.5146554	0.608163	0	2
ClosePublicTransport	17,775	1.008608	0.903268	0	3
StayatHomeRequirements	17,774	2.648532	1.091632	0	4
InternationalTravelControls	17,775	1.406526	0.6967446	0	2
ContactTracing	17,775	53.77538	21.5958	0	100
StringencyIndex	17,778	0.838227	0.8500284	0	2

Source: Oxford COVID-19 Government Response Tracker (OxCGRT).

In addition, we also control for health care and include health expenditures, both in per capita terms and as % of GDP, as well as number of hospital beds, nurses, and physicians per 1,000 people. We consider how healthy is the population with the life expectancy at birth in years and infant mortality rate per 1,000 births. As composite indexes of health care quality we employ Healthcare Access and Quality Index obtained from Institute for Health Metrics and Evaluation and the UHC Service Coverage Index by WHO.

In terms of household financial related data and macroeconomic data (see Table 2), we include in the GVAR: household debt as percentage of household disposable income; household savings; household spending; GDP; exchange; government deficit; share price and long term interest (below we define the data in detail). The OECD countries

that we include in the analysis are: Australia (AUS), Austria (AUT), Belgium (BEL), Brazil (BRA), Canada (CAN), Switzerland (CHE), Chile (CHL), Check Republic (CZE), Germany (DEU), Denmark (DNK), Spain (ESP), Estonia (EST), Finland (FIN), France (FRA), United Kingdom (UK), Greece (GRC), Hungary (HUN), Ireland (IRL), Italy (ITA), Japan (JPN), South Korea (KOR), Lithuania (LTU), Luxemburg (LUX), Latvia (LVA), Mexico (MEX), Netherland (NLD), Norway (NOR), New Zealand (NZL), Poland (POL), Portugal (PRT), Russia (RUS), Slovakia (SVK), Slovenia (SVN), Sweden (SWE), and USA. The period of the sample is from 1981 to 2021 (for 2021 data are provisional.

Table 2: Household and Macroeconomic Data in OECD.

	Obs	Mean	Std.Dev.	Min	Max
Household Debt	690	104.4129	66.4372	-21.78213	339.7779
Household Savings	784	5.284331	7.17107	-39.7524	38.98613
Household Spending	564	544646.2	1496173	572.452	1.40E+07
GDP	1,512	2215284	6428188	3571.07	6.30E+07
Exchange	1,459	146.1827	925.0038	0	13380.8
Gov. Deficit	892	-1.860764	3.80538	-32.1242	17.9505
Share Price	849	58.43929	61.51603	2.70E-09	657.822
Long Term Interest	784	7.706988	13.45292	-0.523833	87.3758

Source: OECD Statistics.

Figure 1 presents household debt in OECD countries in 2020. It is defined as all liabilities of households (including non-profit institutions serving households) that require payments of interest or principal by households to the creditors at a fixed dates in the future. Debt is calculated as the sum of the following liability categories: loans (primarily mortgage loans and consumer credit) and other accounts payable. The indicator is measured as a percentage of net household disposable income. Denmark has the highest debt with Mexico the lowest. The UK household debt is at 148% and comes second highest among G7 countries where Canada reports household debt at 177%. Most OECD countries are above 100%, insinuating the indebtedness of households should be a concern at a global level.

Figure 1: Household debt as percentage of disposable income.

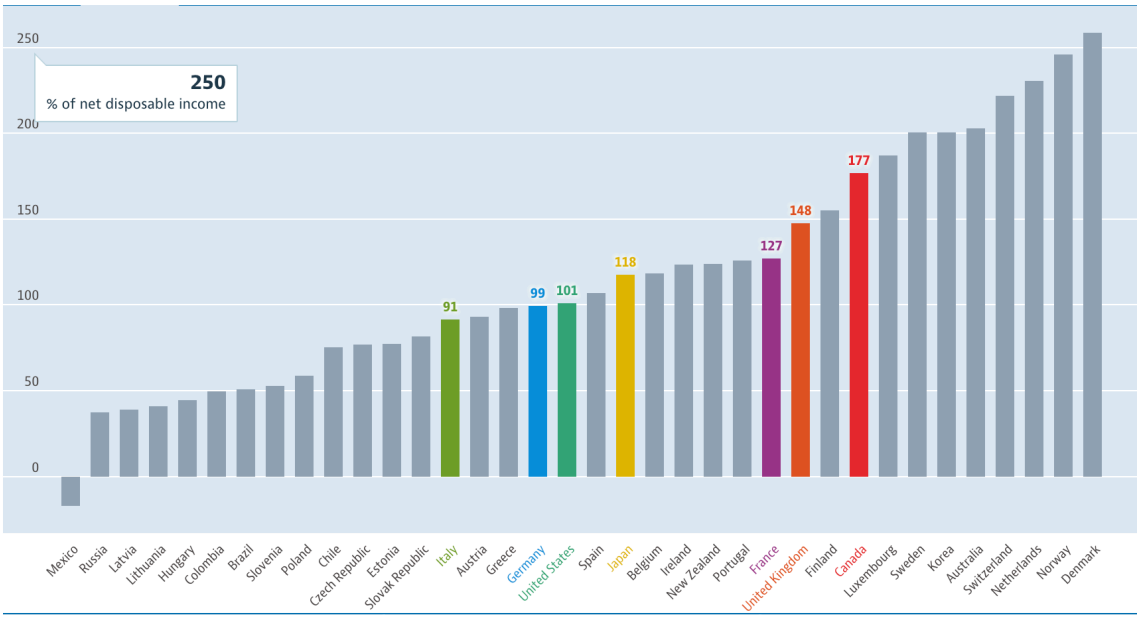

Source: OECD.

In Figure 2 we show the household debt in G7 countries over time. For most countries but USA and Canada, household debt was following an upwards trend as COVID-19 pandemic hit the world economy. As this figure is percentage of disposable income the latter could also explain the upwards trajectory of household debt.

Figure 2: Household debt as percentage of disposable income over time.

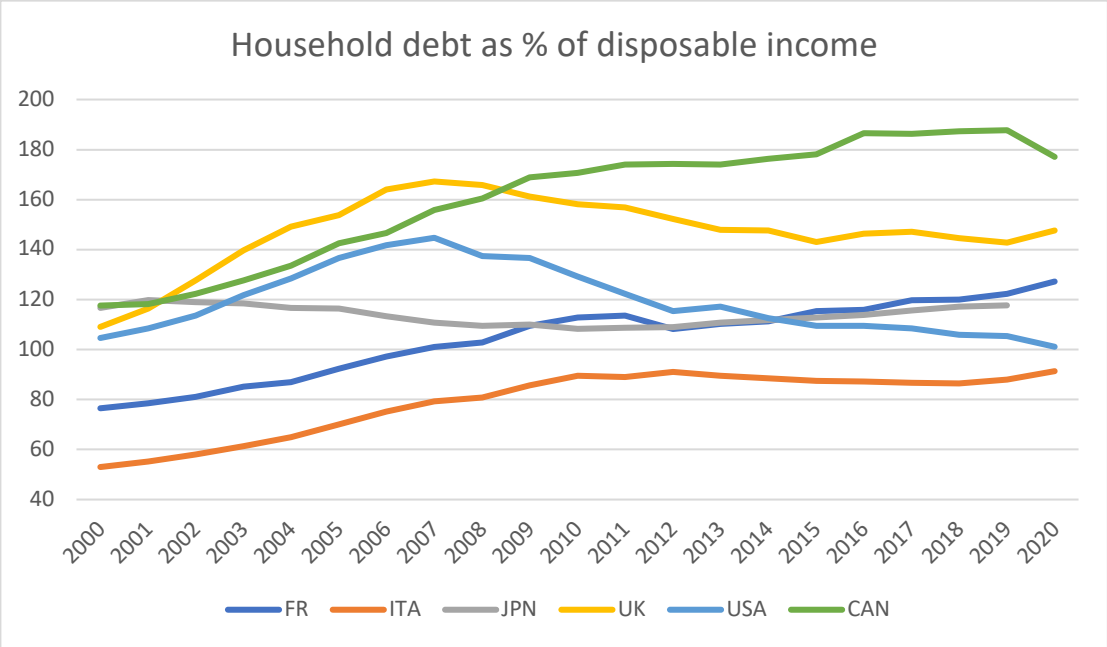

Source: OECD.

Figure 2 reports the household disposable income change from previous year. It reports household disposable income gross, per capita, percentage change, previous period, Q3 2021 or latest available.[2] Note that Figure 2 reports 'real' growth rates adjusted to remove the effects of price changes. It is worth noticing that for US and G7 the real growth of disposable income is negative, while for OECD total is at low levels of 0.17. For UK the real growth rate is low at 0.36, in particular, if compared with Germany's 1.12. The negative real growth rate of disposable income shows that ceteris paribus of the effects COVID-19 households in G7 would face challenges to serve their household debt. The impact of COVID-19 on household debt came at a time that the latter posed uncertainties for the economy. Early indications showed that household debt repayments increase as the pandemic shocked countries across the world. In this paper, we model the impact of shocks related to the pandemic on household debt.

Figure 2: Disposable income, percentage change from previous period.

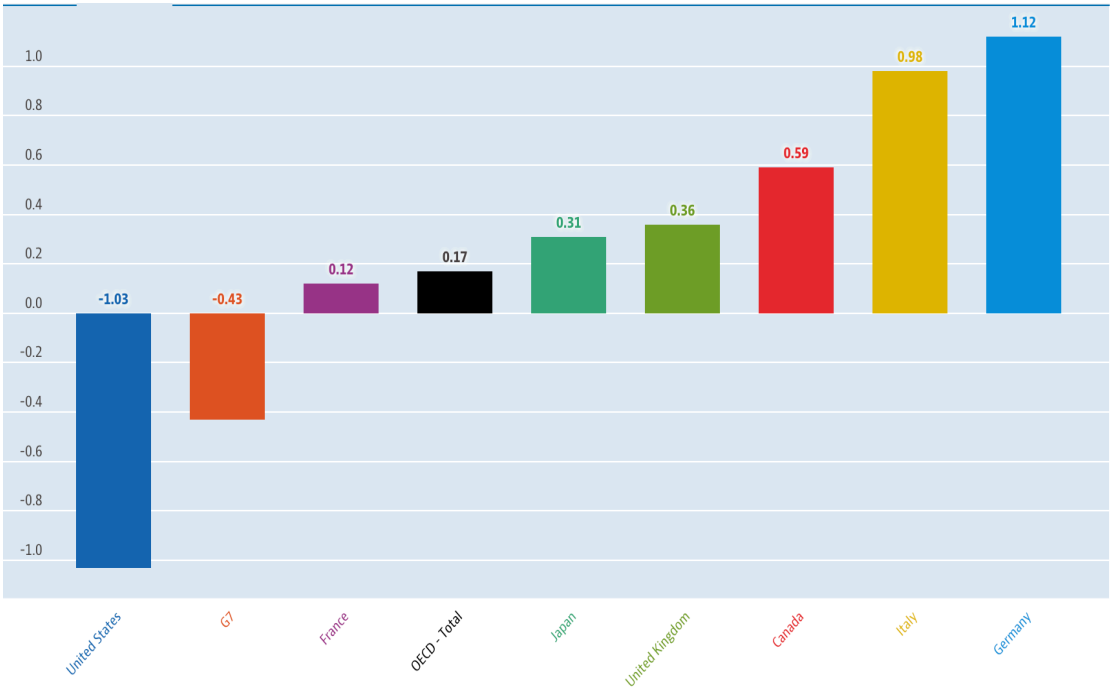

Source: OECD, National Accounts.

[2] OECD data defines household disposable income as income available to households such as wages and salaries, income from self-employment and unincorporated enterprises, income from pensions and other social benefits, and income from financial investments (less any payments of tax, social insurance contributions and interest on financial liabilities) (see OECD, National Accounts). The income is 'gross' and it implies that depreciation costs are not subtracted. Information is also presented for gross household disposable income including social transfers in kind, such as health or education provided for free or at reduced prices by governments and not-for-profit organisations. This indicator is in US dollars per capita at current prices and PPPs. In the System of National Accounts, household disposable income including social transfers in kind is referred to as 'adjusted household disposable income'. All OECD countries compile their data according to the 2008 System of National Accounts (SNA 2008).

In our analysis we employ, net household saving, defined as household net disposable income plus the adjustment for the change in pension entitlements less household final consumption expenditure (households also include non-profit institutions serving households). The adjustment item concerns (mandatory) saving of households, by building up funds in employment-related pension schemes. Household saving is the main domestic source of funds to finance capital investments, a major impetus for long-term economic growth. The net household saving rate represents the total amount of net saving as a percentage of net household disposable income. It thus shows how much households are saving out of current income and how much income they have added to their net wealth. All OECD countries compile their data according to the 2008 System of National Accounts (SNA).

Household spending is also a variable in GVAR and it is defined as the amount of final consumption expenditure made by resident households to meet their everyday needs, such as food, clothing, housing (rent), energy, transport, durable goods (notably cars), health costs, leisure, and miscellaneous services. It is typically around 60% of gross domestic product (GDP) and is therefore an essential variable for economic analysis of demand. Household spending including government transfers (referred to as "actual individual consumption" in national accounts) is equal to households' consumption expenditure plus those expenditures of general government and non-profit institutions serving households (NPISHs) that directly benefit households, such as health care and education. "Housing, water, electricity, gas, and other fuels", one out of the twelve categories distinguished, consist of both actual rentals (for tenants) and imputed rentals (for owner-occupied housing), housing maintenance, as well as costs for water, electricity, gas. Total household spending is measured in million USD (in current prices and Private consumption PPPs), as a percentage of GDP, and in annual growth rates. Household spending including government transfers is measured as a percentage of GDP. Spending in housing is presented as a percentage of household disposable income. All OECD countries compile their data according to the 2008 System of National Accounts (SNA 2008).

4. Empirical results.

4.1 The ANN network: dominant countries.

As a first step in our empirical estimations, we present the OECD weighted network as

in Equation (9). Figure 3 shows this OECD network. To facilitate the presentation of all OECD countries we note countries with numbers by first reporting G7 countries so that: 1 notes the USA, 2 notes the United Kingdom, 3 notes Japan, 4 Germany, 5 France, 6 Italy and 7 Canada. Then the remaining countries are 8 Austria, 9 Australia, 10 Belgium, 11 Brazil (not a member but affiliated), 12 Chile, 13 notes Colombia, 14 notes Czech Republic, 15 Denmark, 16 Estonia, 17 Finland, 18 Greece, 19 notes Hungary, 20 notes Iceland, 21 Ireland, 22 notes Israel, 23 Korea, 24 notes Latvia, 25 notes Lithuania, 26 notes Luxembourg, 27 notes Mexico, 28 notes the Netherlands, 29 notes New Zealand, 30 notes Norway, 31 notes Poland, 32 notes Portugal, 33 notes Slovak Republic, 34 notes Slovenia, 35 notes Spain, 36 notes Sweden, 37 notes Switzerland, 38 notes Turkey. It is worth noting at the outset that the network has a cyclical shape as all nodes are interconnected with each other. Clearly the large economies of OECD like USA, UK, Japan, Germany, France, and Italy are the most important ones in terms of their underlying weight in the network. However, other countries also carry a substantial weight like Belgium, Netherlands and to less degree Brazil. The Figure 3 reveals that the global network is a complex synthesis of multiple interconnections and when it comes to impact of the pandemic the whole world is interconnected without borders.

Figure 3: Network of OECD countries.

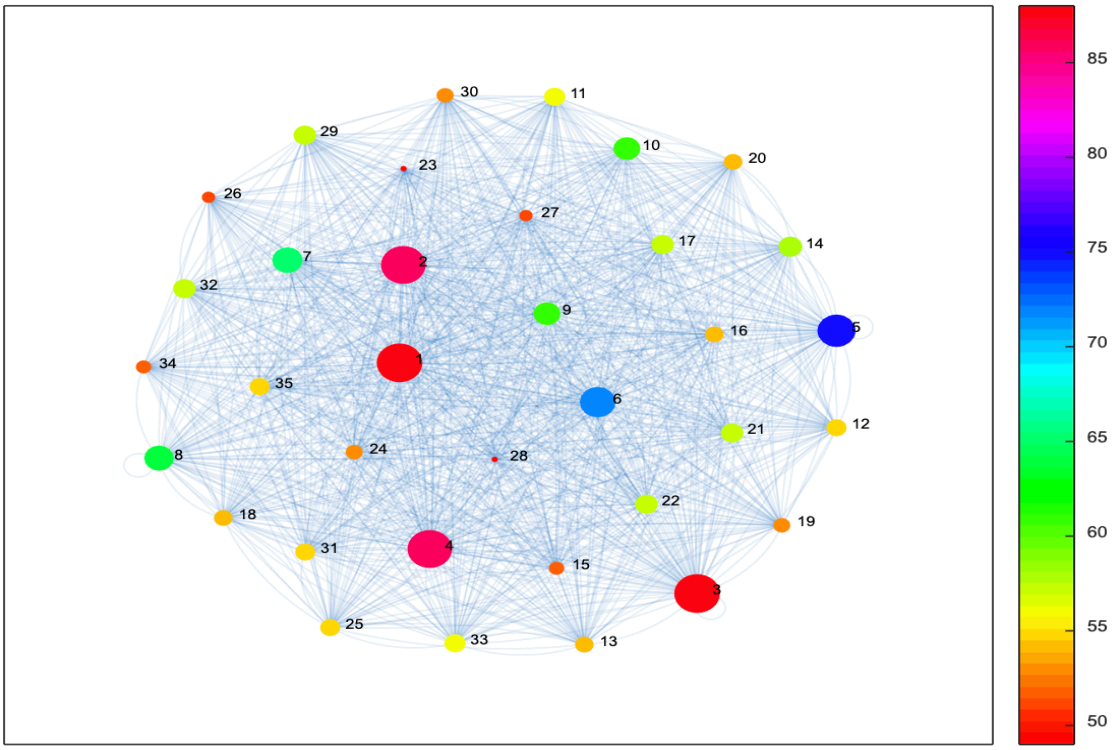

Source: Authors' estimations.

As in Pesaran and Yang (2016), we also report the pervasiveness based on its δ-value of each country's node in the network, see Equation (9). Pesaran and Yang (2016) call these δ-values pervasiveness scores. Table 3 reports δ-values pervasiveness scores for each country. Note that according to Pesaran and Yang (2016) a score below 0.5 will imply very low to none network effect (see also Acemoglou et al. 2012).

Table 3: Degree of pervasiveness

	Pervasiveness	Degree Centrality	Eigenvector Centrality
USA	0.8405	0.9791	0.9753
UK	0.9783	0.9822	0.9443
Japan	0.904	0.8196	0.7359
Germany	0.8696	0.8412	0.8462
France	0.8653	0.9119	0.7905
Italy	0.7532	0.7327	0.7561
Canada	0.8317	0.5298	0.7025
Austria	0.5853	0.1384	0.5545
Australia	0.5182	0.1436	0.0353
Belgium	0.7546	0.1096	0.3872
Brazil	0.6381	0.4591	0.4765
Chile	0.1423	0.0027	0.1919
Colombia	0.5337	0.3884	0.2515
Czech Rep.	0.5283	0.2491	0.7231
Denmark	0.3108	0.0416	0.1652
Estonia	0.4425	0.537	0.5187
Finland	0.1343	0.4519	0.464
Greece	0.0251	0.1675	0.1926
Hungary	0.4594	0.4867	0.0786
Iceland	0.0041	0.4729	0.1994
Ireland	0.574	0.8473	0.2631
Israel	0.122	0.7339	0.4177
Korea	0.535	0.2996	0.1056
Latvia	0.3609	0.0839	0.5205
Lithuania	0.4707	0.2682	0.5121
Luxembourg	0.4891	0.118	0.0433
Mexico	0.1385	0.6833	0.4022
Netherlands	0.7942	0.1346	0.1394
New Zealand	0.2222	0.1277	0.3456
Norway	0.4556	0.5762	0.6884
Poland	0.3257	0.256	0.0625
Portugal	0.3323	0.6644	0.2217
Slovak Rep.	0.3366	0.128	0.0973
Slovenia	0.1292	0.4927	0.1727
Spain	0.2789	0.6169	0.7228

Note: Authors' Estimations.

Table 3 shows that there are several countries with δ-value above 0.8, see USA, UK, Japan, Germany, France, Italy, Canada from G7 but also Belgium, Netherlands, and Brazil to less extent. These values confirmed the findings of the Figure 3 above that shows that there are multiple nodes of importance in the network and that the pandemic has been reaching across the globe. Results show that there are several countries that are dominant and would impact upon the global network. The remaining countries with low δ-value might not be dominant but can assert localised effects in the network.

Table 3 also reports the eigenvector centrality and degree of centrality to identify the dominant country in the network. Note that values below 0.5 would imply that the corresponding country are of significance for the network, while the highest value will imply the dominant country. The results reveal that the USA, closely matched by the UK, are dominant in the network both in terms of degree of centrality and eigenvector centrality. These results may not come as a surprise given then importance of those countries in the global economy.

4.2 Evidence of the impact of COVID-19 infections and COVID-19 deaths on household debt.

In what follows we report the Impulse Response Functions (IRFs) of global panel VAR variables to shocks in COVID-19 confirmed cases and COVID-19 mortality. The first line of diagrams in Figure 3 shows that a shock in confirmed cases will positively affect household debt repayments over the two months period before converging to equilibrium. The response of household savings and household spending is also positive. The case of household savings is of some interest as the response turns negative in month 3 and onwards, but it reverses in month 8 towards positive response underlying the variability in dynamics. The remaining IRFs are consistent with a positive response but for GDP and the return to stock exchange that is negative.

Figure 3: Impact of shocks in confirmed cases to global panel VAR variables.

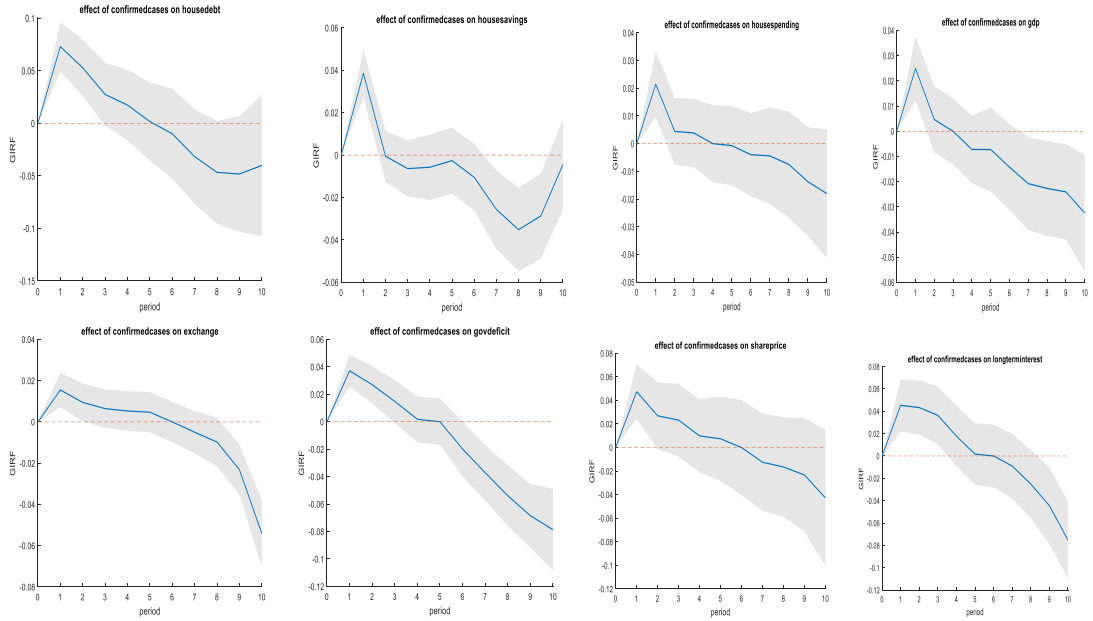

Source: Authors' estimations.

The diagrams in Figure 4 shows that a shock in deaths will positively affect household debt repayments over the two months period before converging to equilibrium. The remaining IRFs are consistent with a positive response but for GDP and the return to stock exchange that is negative.

Figure 4: Impact of shocks in COVID-19 mortality.

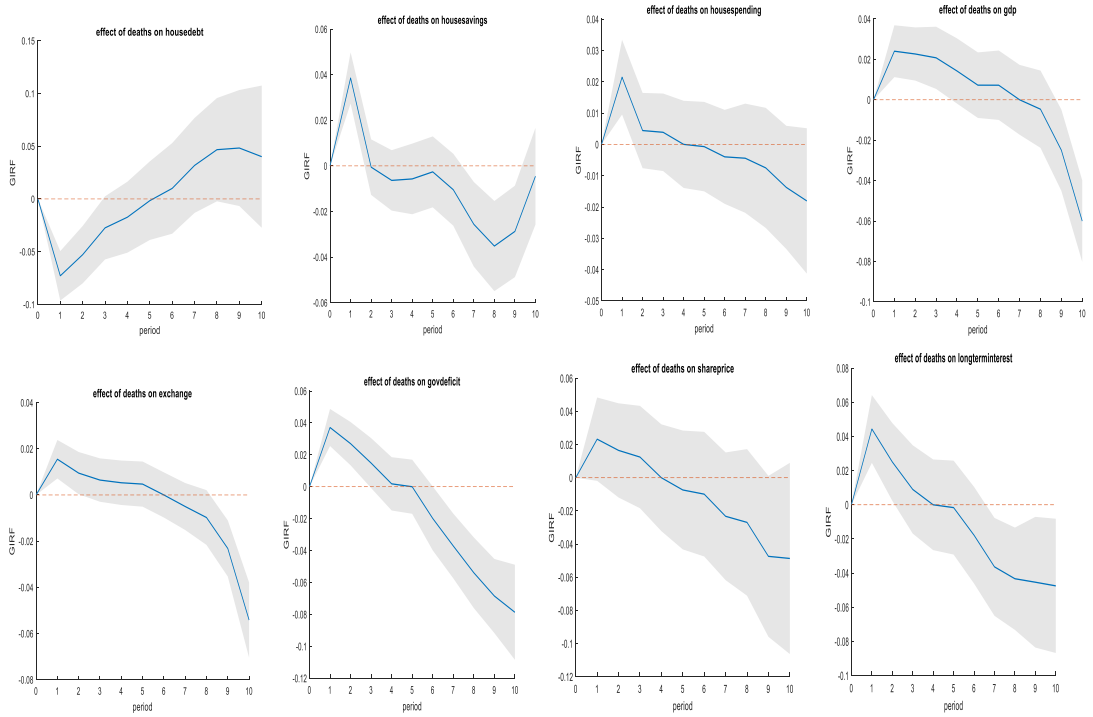

Source: Authors' estimations.

4.3 IRFs of government interventions to control COVID-19.

In the early stages of the pandemic, in spring 2020, governments across the world imposed draconian lock downs and restrictions in economic activity to control the exponential growth of COVID-19 infections. These lock downs scaled down during summer months before returning the following winter of 2020-2021 but also more recently the winter of 2021-2022 as new variants of the virous emerged.

Lockdowns and economic restrictions would have influenced household debt. To examine the response of household debt to such measures we present IRFs. First, we employ the stringency index, which is a function of nine restrictions and lockdowns such as school closures, workplace closures, and travel bans. The index is provided by Oxford COVID-19 Government Response Tracker (OxCGRT) and it is scaled from 0 to 100 with 100 being the strictest restrictions.

In Figure 5 we present the IRFs of the response of household debt to the stringency index (see first graph, in the first line from the left). The response of household debt to stringency is positive in the first month, though statistical significance is not high as the standard errors band is wide. Similarly, it is the picture for household spending while for household savings the response is zero.

Figure 5: Impact of shocks in stringency index to global panel VAR variables.

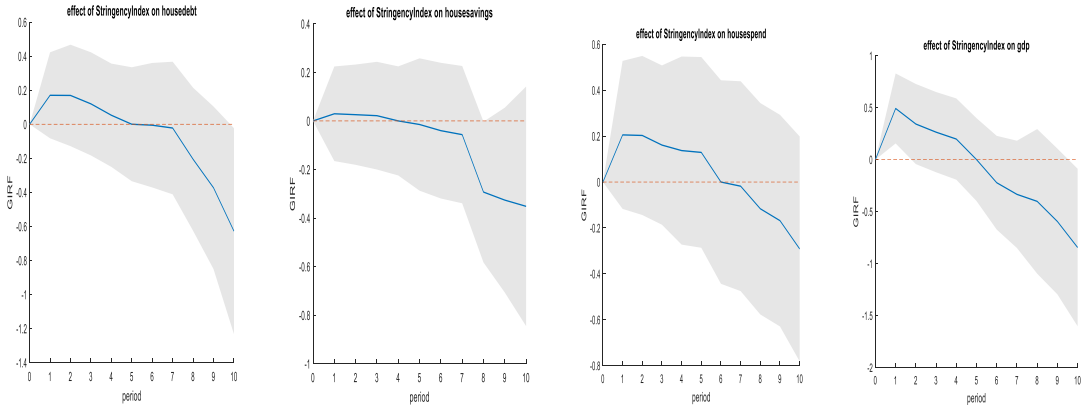

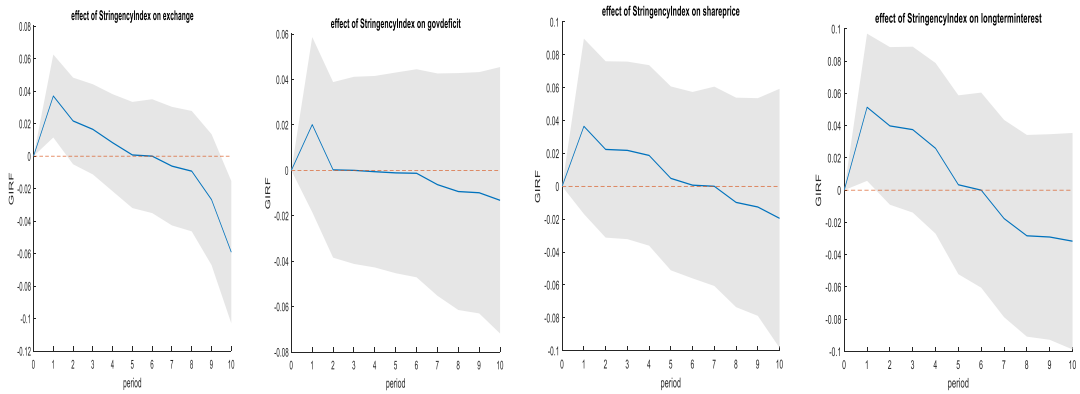

Source: Authors' estimations.

In Figure 6 we report the IRFs of the response of household debt to cancelling of public events. The IRFs are like in Figure 5, and in addition the response of GDP is zero.

Figure 6: Impact of shocks in cancel public events to global panel VAR variables.

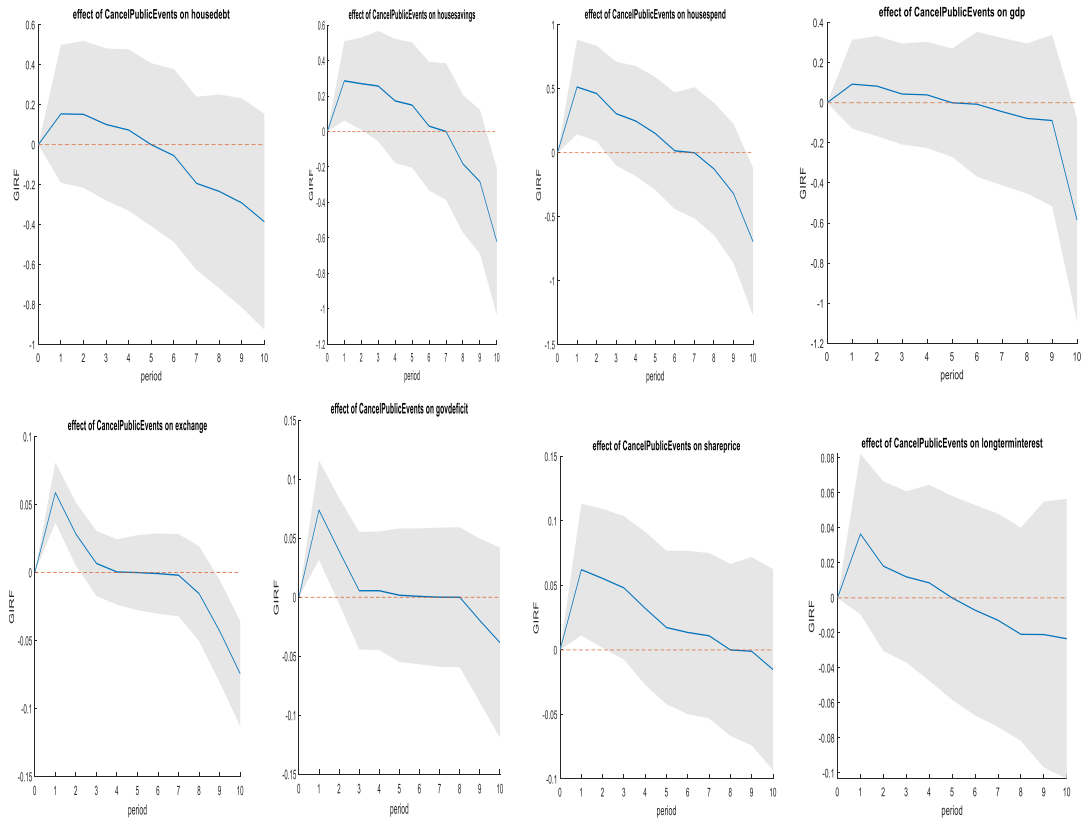

Source: Authors' estimations.

Figures 7 the IRFs of the response of household debt to school closing. These IRFs confirm the above responses.

Figure 7: Impact of shocks in school closing to global panel VAR variables.

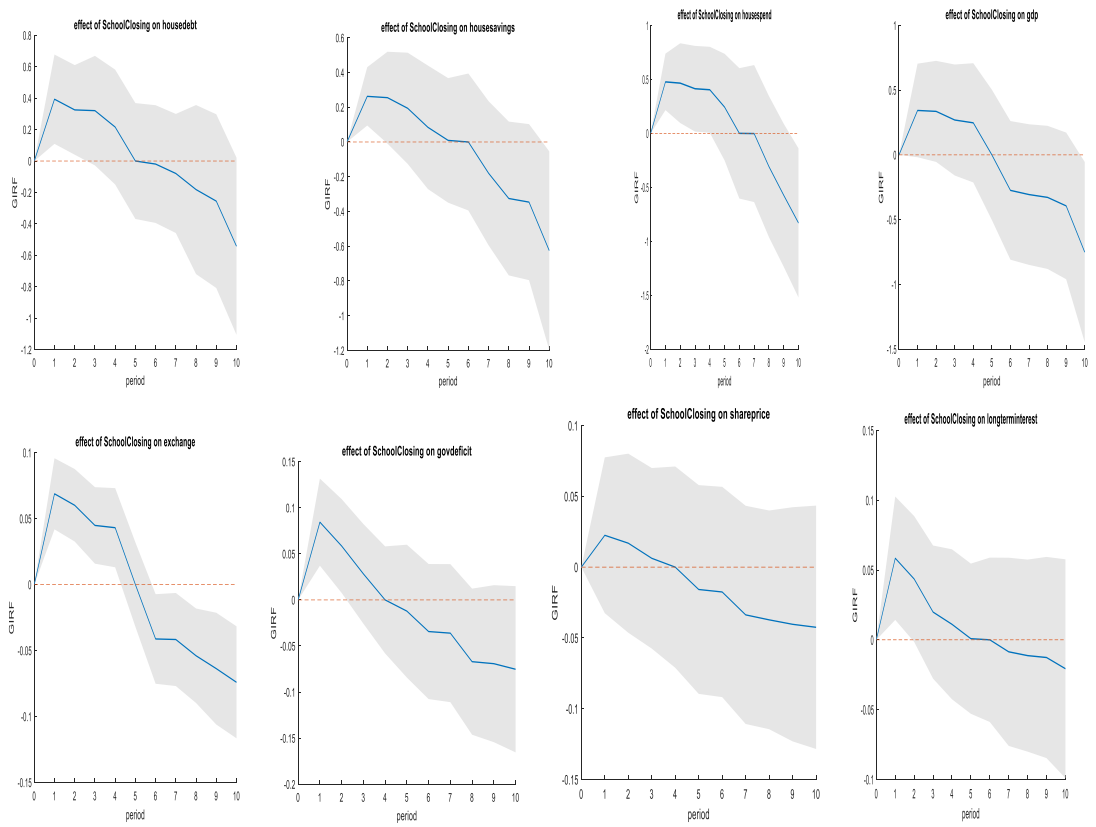

Source: Authors' estimations.

Lastly, Figures 8 present the IRFs of the response of household debt to stay at home advise respectively. These IRFs confirm the above responses.

Figure 8: Impact of shocks in stay at home to global panel VAR variables.

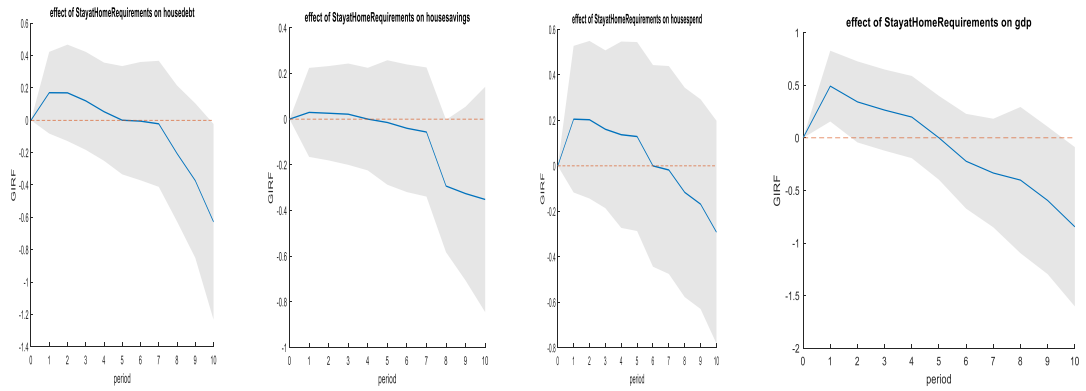

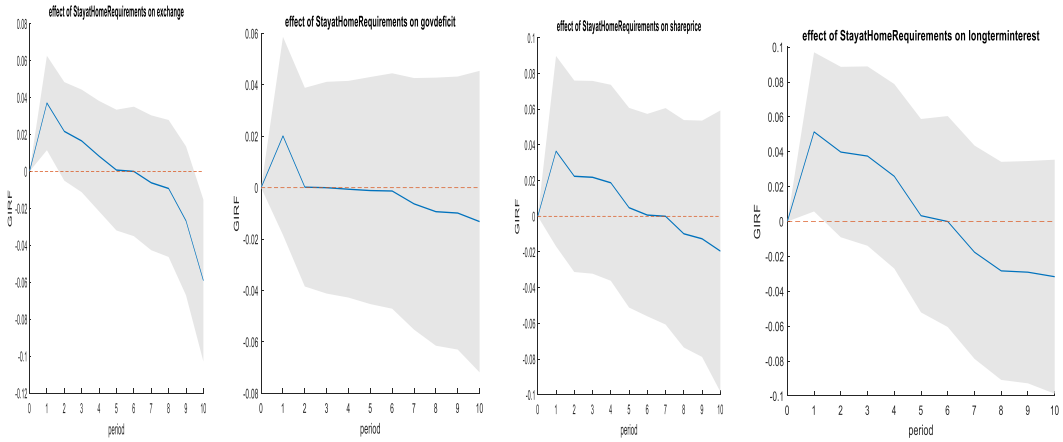

Source: Authors' estimations.

4.4 Evidence of the impact of pharmaceutical interventions: vaccination, testing, contact tracing.

Next, we report the IRFs from medical interventions to combat COVID-19 like testing, vaccination, and contact tracing. We begin by reporting the in Figure 9 responses to vaccinations. Interestingly, vaccination programs negatively affect household debt repayments, suggesting that although COVID-19 would have initially enhanced debt repayments as uncertainty was increasing the rapid development of vaccines and their deployment would restore household confidence towards household debt. On the other hand, the response of household savings and household spending is also positive. The case of household savings is of some interest as the response turns negative in month 3 and onwards, but it reverses in month 8 towards positive response underlying the variability in dynamics. The remaining IRFs are consistent with a positive response but for GDP and the return to stock exchange that is negative.

Figure 9: Impact of shocks in vaccination to global panel VAR variables.

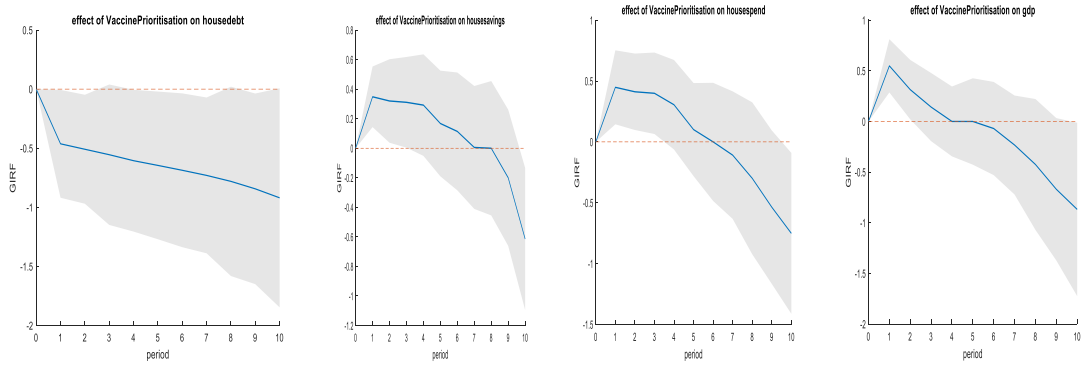

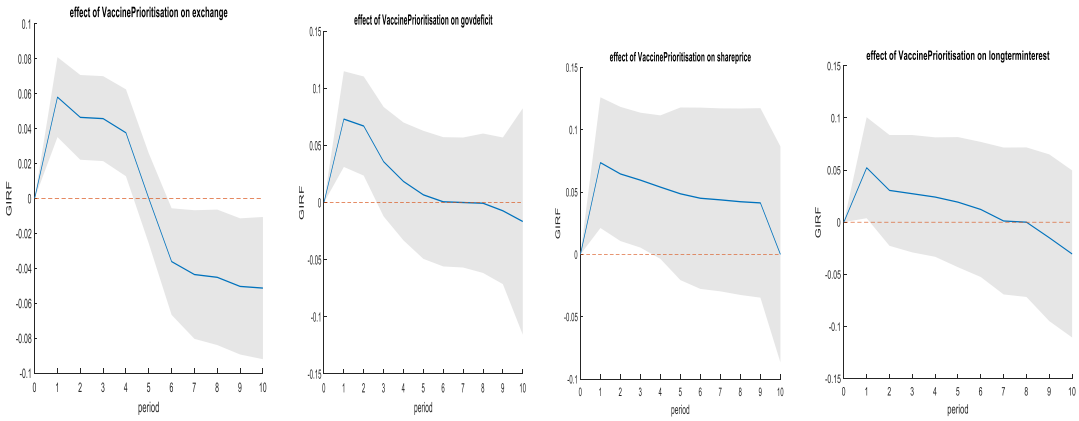

Source: Authors' estimations.

Figures 10 present the IRFs of the response of household debt to testing. These IRFs in these Figures are broadly consistent with the IRFs in Figure 9.

Figure 10: Impact of shocks in testing to global panel VAR variables.

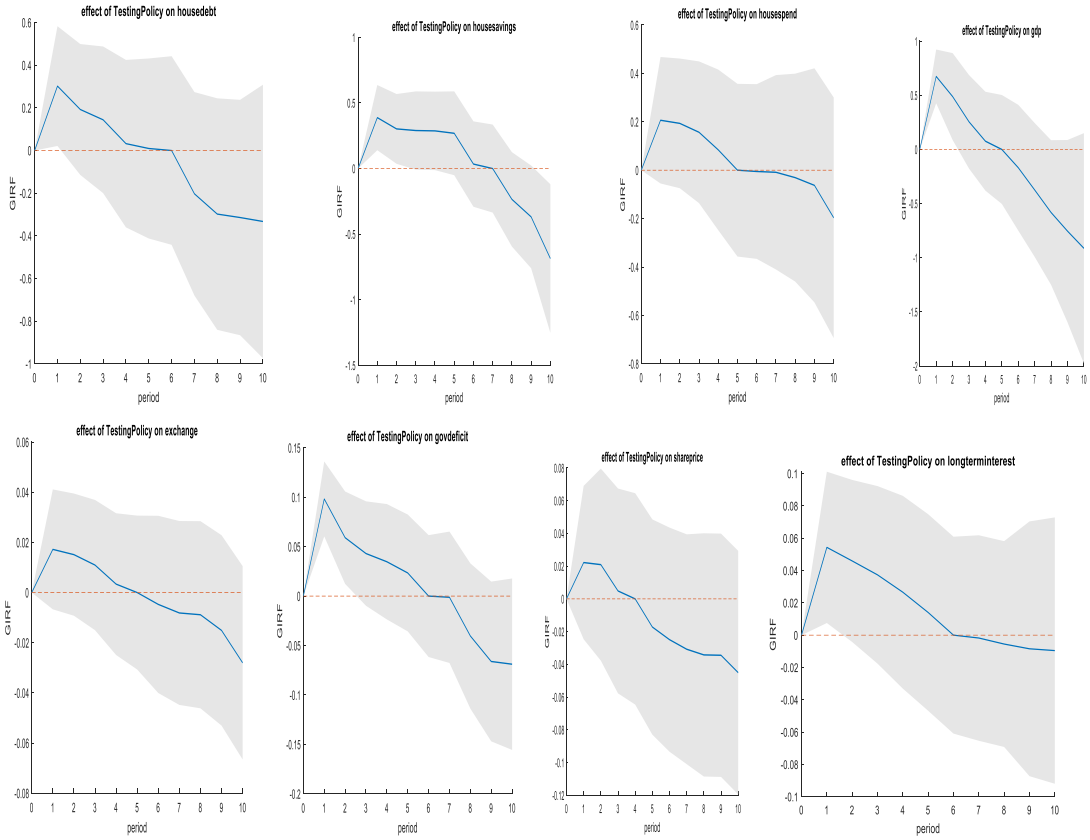

Source: Authors' estimations.

Figures 11 present the IRFs of the response of household debt to contact tracing. These IRFs in these Figures are broadly consistent with the IRFs in Figure 9.

Figure 11: Impact of shocks in contact tracing to global panel VAR variables.

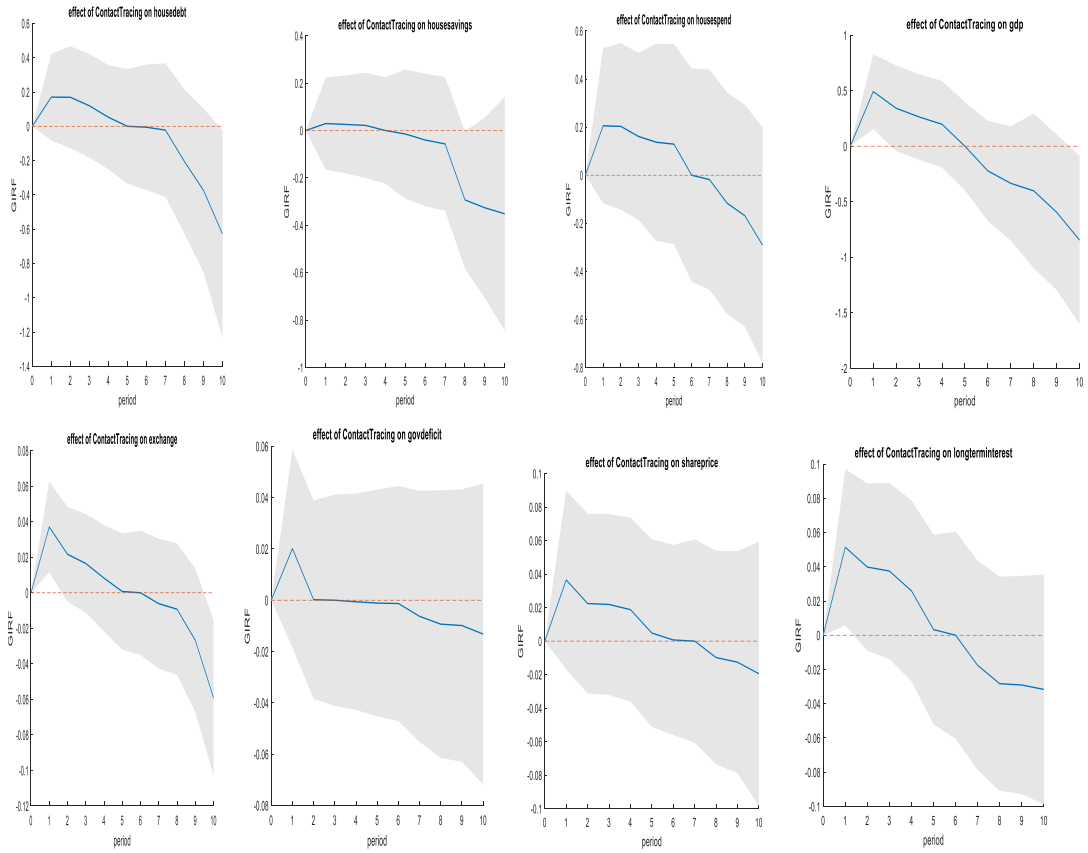

Source: Authors' estimations.

5. Conclusions

The reported δ-values that capture the dominance of each individual country in the network reveal that dominant countries are UK, USA, and Japan within the network, but Belgium, Netherlands and Brazil also have high dominance. The GVAR results show that household debt positively responds to COVID-19 infections and mortality as well as lockdowns, though this response is valid in the short term. However, vaccinations and testing appear to negatively affect household debt. Lockdown measures such as stay-at-home advice, and closing schools, all have a positive impact on household debt, though they are of transitory nature.

It appears that the dominant countries in the underlying networks are the USA, UK and the remaining G7 countries. We reveal that there are a plethora of nodes and interconnections across countries when it comes to pandemic the global economy is highly interconnected. Given the results of the network, and in terms of policy

implications, as global coordinated action is required as an effective way to deal with the pandemic.

Compliance with Ethical Standards:

Funding: This study was funded by ERC ADG 2016 - GA 740272 and ESRC ES/V015826/1.

Conflict of Interest: Emmanuel Mamatzakis declares that he has no conflict of interest. Mike Tsionas declares that he has no conflict of interest. Steven Ongena declares that he has no conflict of interest.

Ethical approval: This article does not contain any studies with human participants or animals performed by any of the authors.

References

Almon, S. (1965). The distributed lag between capital appropriations and expenditures. Econometrica 33 (1), 178–196.

Andrieu, C., Doucet, A., Holenstein, R., 2010. Particle Markov chain Monte Carlo methods (with discussion). Journal of the Royal Statistical Society Series B 72 (2), 1–33.

Bair, E., T. Hastie, D. Paul, R. Tibshirani (2006). Prediction by Supervised Principal Components. Journal of the American Statistical Association 101 (473), 119–137.

Carriero, A., Clark, T. and Marcellino, M. (2015). Large vector autoregressions with asymmetric priors and time varying volatilities, manuscript.

Carvalho, V.M., S. Hansen, A. Ortiz, J.R. Garcia, T. Rodrigo, S. Rodriguez Mora, P. Ruiz de Aguirre, (2020). Tracking the COVID-19 Crisis with High-Resolution Transaction Data, CEPR Discussion Paper Series No. DP14642.

Chetty, R., J.N. Friedman, N. Hendren, M. Stepner (2020). How Did COVID-19 and Stabilization Policies Affect Spending and Employment? A New Real-Time Economic Tracker Based on Private Sector Data, NBER Working Paper Series No.27431.

Chopin, N., Singh, S.S., 2013. On the particle Gibbs sampler. Working paper, ENSAE. http://arxiv.org/abs/1304.1887.

Creal, D.D., 2012. A survey of sequential Monte Carlo methods for economics and finance. Econometric Reviews 31 (3), 245–296.

Creal, D., and R. Tsay (2015). High dimensional dynamic stochastic copula models. Journal of Econometrics 189 (2), 335–345.

Christelis, D., Georgarakos, D., Jappelli, T., Kenny. G., (2020). The Covid 19 crisis and consumption: survey evidence from six EU countries, ECB Working Paper no.

2507.

DiCiccio, T. J., Kass, R. E., Raftery, A., Wasserman, L. (1997), Computing Bayes factors by combining simulation and asymptotic approximations. Journal of the American Statistical Association 92 903–915.

Eisenstat, E., Chan, J. and Strachan, R. (2016). Stochastic model specification search for time-varying parameter VARs, Econometric Reviews 35 (8-10), 1638–1665.

Franklin, Jeremy, Georgina Green, Lindsey Rice-Jones, Sarah Venables and Teresa Wukovits-Votzi (2021). Household debt and Covid, Quarterly Bulletin Q2, Bank of England.

Georgarakos, Dimitris and Geoff Kenny, (2022). Household spending and fiscal support during the COVID-19 pandemic: Insights from a new consumer survey, Journal of Monetary Economics, available on-line 25 February.

Geweke, J. (1999), Using simulation methods for Bayesian econometric models: inference, development, and communication. Econometric Reviews 18 (1), 1–73.

Ghysels, E. (2016). Macroeconomics and the reality of mixed frequency data. Journal of Econometrics, 193 (2), 294–314.

Girolami, M., & B. Calderhead (2011). Riemann manifold Langevin and Hamiltonian Monte Carlo methods. Journal of the Royal Statistical Society Series B 73 (2), 123–214.

Godsill, S.J., Doucet, A., West, M., 2004. Monte Carlo smoothing for nonlinear time series. Journal of the American Statistical Association 99 (465), 156–168.

Khalaf, L., M. Kichian, C.J. Saunders et al., (2021). Dynamic panels with MIDAS covariates: Nonlinearity, estimation and fit. Journal of Econometrics, 220 (2), 589–605.

Koop, G., D., Korobilis and D. Pettenuzzo (2017). Bayesian Compressed Vector Autoregressions, manuscript.

Koop, G., Pesaran, M.H. & Potter, S. (1996). Impulse Response Analysis in Nonlinear Multivariate Models. Journal of Econometrics, 74: 119-147.

Kubota, So, Koichiro, Onishi, Yuta Toyama, (2021). Consumption responses to COVID-19 payments: Evidence from a natural experiment and bank account data, Journal of Economic Behavior & Organization, Volume 188, Pages 1-17,

OECD, Statistics, various data sets, Paris.

OECD (2020). Evaluating the initial impact of COVID-19 containment measures on economic activity, Paris.

Pesaran, M. H. & Shin, Y. (1998). Generalized Impulse Response Analysis in Linear

Multivariate Models. Economics Letters, 58: 17-29.

Primiceri, G., (2005). Time varying structural vector autoregressions and monetary policy. Review of Economic Studies, 72, 821-852.

Roth, J. and Wohlfart (2020). How Do Expectations about the macroeconomy affect personal expectations and behavior? Rev. Econ. Stat., 102 (4), pp. 731-748.

Roth, S., Settele, and J. Wohlfart (2021). Beliefs about public debt and the demand for government spending, J. Econom. forthcoming.

Zabai, Anna (2020). How are household finances holding up against the Covid-19 shock? BIS Bulletin, No 22, 15 June.

Appendix

A.1. The Creal and Tsay (2015) procedure

We use a recent advance in sequential Monte Carlo methods known as the particle Gibbs (PG) sampler, see Andrieu et al. (2010). The algorithm allows us to draw paths of the state variables in large blocks. Particle filtering is a simulation-based algorithm that sequentially approximates continuous, marginal distributions using discrete distributions. This is performed by using a set of support points called ''particles'' and probability masses; see Creal (2012) for a review. The PG sampler draws a single path of the latent or state variables from this discrete approximation. As the number of particles M goes to infinity, the PG sampler draws from the exact full conditional distribution. As mentioned in Creal and Tsay (2015, p. 339): "The PG sampler is a standard Gibbs sampler but defined on an extended probability space that includes all the random variables that are generated by a particle filter. Implementation of the PG sampler is different than a standard particle filter due to the ''conditional'' resampling algorithm used in the last step. Specifically, for draws from the particle filter to be a valid Markov transition kernel on the extended probability space, Andrieu et al. (2010) note that there must be positive probability of sampling the existing path of the state variables that were drawn at the previous iteration. The pre-existing path must survive the resampling steps of the particle filter. The conditional resampling step within the algorithm forces this path to be resampled at least once. We use the conditional multinomial resampling algorithm from Andrieu et al. (2010), although other resampling algorithms exist, see Chopin and Singh (2013)." We follow Creal and Tsay (2015). Suppose the posterior is $p(\theta, \Lambda_{1:T}|\boldsymbol{y}_{1:T})$ where $\Lambda_{1:T}$ denotes the latent variables whose prior can be described by $p(\Lambda_t|\Lambda_{t-1}, \theta)$. In the PG sampler we can draw the structural parameters $\theta|\Lambda_{1:T}, \boldsymbol{y}_{1:T}$ as usual, from their posterior conditional distributions. This is important because, in this way, we can avoid mixture approximations or other Monte Carlo procedures that need considerable tuning and may not have good convergence properties. As such posterior conditional distributions, we omit the details and focus on drawing the latent variables. Suppose we have $\Lambda_{1:T}^{(1)}$ from the previous iteration. The particle filtering procedure consists of two phases.

Phase I: Forward filtering (Andrieu et al., 2010).

- Draw a proposal $\Lambda_{i,t}^{(m)}$ from an importance density $q(\Lambda_{i,t}|\Lambda_{i,t-1}^{(m)},\theta), m = 2, \dots, M$.
- Compute the importance weights:

$$w_{i,t}^{(m)} = \frac{p(y_{i,t};\Lambda_{i,t}^{(m)},\theta)p(\Lambda_{i,t}^{(m)}|\Lambda_{i,t-1}^{(m)},\theta)}{q(\Lambda_{i,t}|\Lambda_{i,t-1}^{(m)},\theta)}, m = 1, \dots, M. \quad \text{(A.1)}$$

- Normalize the weights: $\widetilde{w}_{i,t}^{(m)} = \frac{w_{it}^{(m)}}{\sum_{m'=1}^{M} w_{it}^{(m')}}, m = 1, \dots, M$.
- Resample the particles $\{\Lambda_{i,t}^{(m)}, m = 1, \dots, M\}$ with probabilities $\{\widetilde{w}_{i,t}^{(m)}, m = 1, \dots, M\}$.

In the original PG sampler, the particles are stored for $t = 1, \dots, T$ and a single trajectory is sampled using the probabilities from the last iteration. An improvement upon the original PG sampler was proposed by Whiteley (2010), who suggested drawing the path of the latent variables from the particle approximation using the backwards sampling algorithm of Godsill et al. (2004). In the forwards pass, we store the normalized weights and particles, and we draw a path of the latent variables as we detail below (the draws are from a discrete distribution).

Phase II: Backward filtering (Chopin and Singh, 2013, Godsill et al., 2004).

- At time $t = T$ draw a particle $\Lambda_{i,T}^{*} = \Lambda_{i,T}^{(m)}$.
- Compute the backward weights: $w_{t|T}^{(m)} \propto \widetilde{w}_{t}^{(m)} p(\Lambda_{i,t+1}^{*}|\Lambda_{i,t}^{(m)},\theta)$.
- Normalize the weights: $\widetilde{w}_{t|T}^{(m)} = \frac{w_{t|T}^{(m)}}{\sum_{m'=1}^{M} w_{t|T}^{(m')}}, m = 1, \dots, M$.
- Draw a particle $\Lambda_{i,t}^{*} = \Lambda_{i,t}^{(m)}$ with probability $\widetilde{w}_{t|T}^{(m)}$.

Therefore, $\Lambda_{i,1:T}^{*} = \{\Lambda_{i1}^{*}, \dots, \Lambda_{iT}^{*}\}$ is a draw from the full conditional distribution. The backwards step often results in dramatic improvements in computational efficiency. For example, Creal and Tsay (2015) find that $M = 100$ particles is enough. There remains the problem of selecting an importance density $q(\Lambda_{i,t}|\Lambda_{i,t-1},\theta)$. We use an importance

density implicitly defined by $\Lambda_{i,t} = a_{i,t} + \sum_{p=1}^{P} b_{i,t}\,\Lambda_{i,t-1}^{p} + h_{i,t}\xi_{i,t}$ where $\xi_{i,t}$ follows a standard (zero location and unit scale) Student-t distribution with $\nu = 5$ degrees of freedom. That is, we use polynomials in $\Lambda_{i,t-1}$ of order P. We select the parameters $a_{i,t}, b_{i,t}$ and $h_{i,t}$ during the burn-in phase (using $P = 1$ and $P = 2$) so that the weights $\{\widetilde{w}_{i,t}^{(m)}, m = 1, \dots, M\}$ and $\{\widetilde{w}_{t|T}^{(m)}, m = 1, \dots, M\}$ are approximately not too far from a uniform distribution. Chopin and Singh (2013) have analyzed the theoretical properties of the PG sampler and proved that the sampler is uniformly ergodic. They also prove that the PG sampler with backwards sampling strictly dominates the original PG sampler in terms of asymptotic efficiency.

Alternatively, when the dimension of the state vector is large, we can draw $\Lambda_{i,1:T}$, conditional on all other paths $\Lambda_{-i,1:T}$ that are not path i. Therefore, we can draw from the full conditional distribution $p(\Lambda_{i,1:T}|\Lambda_{-i,1:T}, \boldsymbol{y}_{1:T}, \theta)$.

A.2. The Girolami and Calderhead (2011) procedure

We use a Girolami and Calderhead (2012, GC) algorithm to update draws for a parameter $\boldsymbol{\theta}$ which in our case is $\boldsymbol{\beta}$. The algorithm uses local information about both the gradient and the Hessian of the log-posterior conditional of $\boldsymbol{\theta}$ at the existing draw. A Metropolis test is again used for accepting the candidate so generated, but the GC algorithm moves considerably faster relative to our naive scheme previously described. The GC algorithm is started at the first-stage GMM estimator and MCMC is run until convergence. It has been found that the GC algorithm performs vastly superior relative to the standard MH algorithm and autocorrelations are much smaller. Suppose $L(\boldsymbol{\theta}) = \log\, p\,(\boldsymbol{\theta}|\boldsymbol{X})$ is used to denote for simplicity the log posterior of $\boldsymbol{\theta}$.

Moreover, define

$$\boldsymbol{G}(\boldsymbol{\theta}) = \text{est. cov}\frac{\partial}{\partial\boldsymbol{\theta}}\log\, p\,(\boldsymbol{X}|\boldsymbol{\theta}) \tag{A.2}$$

the empirical counterpart of

$$\boldsymbol{G}_o(\boldsymbol{\theta}) = -E_{Y|\boldsymbol{\theta}}\frac{\partial^2}{\partial\boldsymbol{\theta}\partial\boldsymbol{\theta}'}\log\, p\,(\boldsymbol{X}|\boldsymbol{\theta}) \tag{A.3}$$

The Langevin diffusion is given by the following stochastic differential equation:

$$d\boldsymbol{\theta}(t) = \frac{1}{2}\tilde{\nabla}_{\boldsymbol{\theta}} L\{\boldsymbol{\theta}(t)\}dt + d\boldsymbol{B}(t) \tag{A.4}$$

where

$$\tilde{\nabla}_{\boldsymbol{\theta}} L\{\boldsymbol{\theta}(t)\} = -\boldsymbol{G}^{-1}\{\boldsymbol{\theta}(t)\} \cdot \nabla_{\boldsymbol{\theta}} L\{\boldsymbol{\theta}(t)\} \tag{A.5}$$

is the so called "natural gradient" of the Riemann manifold generated by the log posterior.

The elements of the Brownian motion are

$$\begin{aligned} &\boldsymbol{G}^{-1}\{\boldsymbol{\theta}(t)\} d\boldsymbol{B}_i(t) \\ &= |\boldsymbol{G}\{\boldsymbol{\theta}(t)\}|^{-1/2} \sum_{j=1}^{K_\beta} \frac{\partial}{\partial \boldsymbol{\theta}} \left[mbolG^{-1}\{\boldsymbol{\theta}(t)\}_{ij} |\boldsymbol{G}\{\boldsymbol{\theta}(t)\}|^{1/2} \right] dt \\ &\qquad + \left[\sqrt{\boldsymbol{G}\{\boldsymbol{\theta}(t)\}} d\boldsymbol{B}(t) \right]_i \end{aligned} \tag{A.6}$$

The discrete form of the stochastic differential equation provides a proposal as follows:

$$\begin{aligned} &\tilde{\boldsymbol{\theta}}_i \\ &= \boldsymbol{\theta}_i^o + \frac{\varepsilon^2}{2} \{\boldsymbol{G}^{-1}(\boldsymbol{\theta}^o) \nabla_{\boldsymbol{\theta}} L(\boldsymbol{\theta}^o)\}_i \qquad + \frac{\varepsilon^2}{2} \sum_{j=1}^{K_\theta} \{\boldsymbol{G}^{-1}(\boldsymbol{\theta}^o)\}_{ij} \operatorname{tr} \left\{ \boldsymbol{G}^{-1}(\boldsymbol{\theta}^o) \frac{\partial \boldsymbol{G}(\boldsymbol{\theta}}{\partial \boldsymbol{\theta}} \right. \\ &- \varepsilon^2 \sum_{j=1}^{K_\theta} \left\{ \boldsymbol{G}^{-1}(\boldsymbol{\theta}^o) \frac{\partial \boldsymbol{G}(\boldsymbol{\theta}^o)}{\partial \boldsymbol{\theta}_j} \boldsymbol{G}^{-1}(\boldsymbol{\theta}^o) \right. + \left\{ \varepsilon \sqrt{\boldsymbol{G}^{-1}(\boldsymbol{\theta}^o)} \boldsymbol{\xi}^o \right\}_i \\ &\qquad = \boldsymbol{\mu}(\boldsymbol{\theta}^o, \varepsilon)_i + \left\{ \varepsilon \sqrt{\boldsymbol{G}^{-1}(\boldsymbol{\theta}^o)} \boldsymbol{\xi}^o \right\}_i, \end{aligned}$$

where $\boldsymbol{\beta}^o$ is the current draw.

The proposal density is

$$q(\tilde{\boldsymbol{\theta}} | \boldsymbol{\theta}^o) = \mathcal{N}_{K_\theta}\left(\tilde{\boldsymbol{\theta}}, \varepsilon^2 \boldsymbol{G}^{-1}(\boldsymbol{\theta}^o)\right), \tag{A.7}$$

and convergence to the invariant distribution is ensured by using the standard form Metropolis-Hastings probability

$$\min \left\{ 1, \frac{p(\tilde{\boldsymbol{\theta}} | \cdot, Y) q(\boldsymbol{\theta}^o | \tilde{\boldsymbol{\theta}})}{p(\boldsymbol{\theta}^o | \cdot, Y) q(\tilde{\boldsymbol{\theta}} | \boldsymbol{a}^o)} \right\}. \tag{A.8}$$